ARTICLES

Temperature Dependence of Solvation Dynamics in Alkylcyanobiphenyls

J. Rau,[†] C. Ferrante,[#] E. Kneuper,[†] F. W. Deeg,*[,†] and C. Bräuchle[†]

Chemistry Department, Ludwig-Maximilians-Universität München, Butenandtstrasse 5-13, Building E, D-81377 München, Germany, and Dipartimento di Chimica Fisica, Via Loredan 2, I-35131 Padova, Italy

Received: October 17, 2000; In Final Form: March 23, 2001

Earlier investigations of the solvation dynamics of the cationic dye rhodamine 700 in the isotropic phase of the nematogenic substance octylcyanobiphenyl (Rau, J., Ferrante, C., Deeg, F. W., Bräuchle, C. *J. Phys. Chem. B* **1999**, *103*, 931) have shown that in this liquid two different contributions to the solvation dynamics exist. The slower one can be explained in terms of polar solvation, while the second one is not yet fully understood. The latter one is temperature independent from the nematic−isotropic phase transition temperature up to 20 K above the transition temperature. We present in this paper two different approaches to a better understanding of the solvation dynamics of the alkylcyanobiphenyls. First, it was investigated if a different member of the family of the alkylcyanobiphenyls, butylcyanobiphenyl, exhibits similar dynamic behavior. To check the possible influence of the probe chromophore, the neutral dye coumarin 153 was dissolved in octylcyanobiphenyl for a second set of measurements. The time-resolved dynamic Stokes shift $S(t)$ was measured above the nematic−isotropic phase transition. Butylcyanobiphenyl with the probe chromophore rhodamine 700 and octylcyanobiphenyl with coumarin 153 show qualitatively the same contributions as found in the solution of rhodamine 700 in octylcyanobiphenyl. From this, we conclude that the peculiar dynamics observed is characteristic for the whole family of the alkylcyanobiphenyls and not only for a special system of probe molecule and liquid. In addition to the solvation dynamics the temperature dependence of the rotational relaxation times of the dye molecules was recorded.

Introduction

Mesogenic liquid crystalline materials have been investigated with various techniques[1−4] in the isotropic phase close to the nematic−isotropic phase transition. This transition has been thoroughly studied and shows a weakly first-order behavior. Consequently, approaching it some of the physical parameters describing the dynamics in these complex liquids show a critical dependence as a function of the temperature, which has been well described through the Landau−de Gennes theory.[5] Examples for them are long-range orientational correlation lengths[6,7] or the reorientational dynamics.[8,9] The influence of these so-called pseudonematic domains formed by several thousand molecules have been observed in dynamical optical Kerr effect (OKE) experiments for the liquid crystalline family of alkylcyanobiphenyls,[8,10] which we also investigate in this work. Dielectric measurements[11−13] in contrast do not show this critical temperature dependence. This can be explained if one considers that the dipole moments of the molecules are equally distributed over the two orientations along the director of the pseudonematic domains; therefore, the average dipole moment in these domains vanishes.

A different approach in understanding the dynamics of liquid crystals is through solvation dynamics, provided that the solute will affect the nematogenic structure of the surrounding liquid in a negligible manner. Solvation dynamics can be measured through the observation of the time-resolved shift of the fluorescence spectrum of solvated dye molecules.[14−17] The investigation of the temperature dependence of the solvation dynamics experienced by the probe molecule rhodamine 700 (Rh700) in the isotropic phase of the liquid crystal octylcyanobiphenyl (8CB) did not show any critical process,[18] so the reorientation of the pseudonematic domains has not been observed by this method. It is not yet clear whether this behavior results from the fact that this collective relaxation dynamics is too slow to be observed during the fluorescence lifetime, or if there is no coupling between the probe molecules and the process of the relaxation of the pseudonematic domains. Other independent experiments together with theoretical work[19] on the liquid crystalline mixture ZLI-1167 with the probe chromophore coumarin 502 showed that the solvation dynamics could be satisfactorily described by polar solvation, where the reaction of the solvent to an electronic change in the probe molecule after excitation is depicted in terms of dielectric relaxation.[20−22] Our previous measurements[18] on Rh700 in 8CB confirm these findings. We detected a process showing the predicted viscosity/temperature dependence and the absolute value of the time constant is in the range expected for polar solvation in this liquid.

Besides this temperature-dependent component the system Rh700 in 8CB is characterized by a second component showing

* To whom correspondence should be addressed. E-Mail: Fred-Walter.Deeg@cup.uni-muenchen.de.
[†] Ludwig-Maximilians-Universität.
[#] Dipartimento di Chimica Fisica.

10.1021/jp003828g CCC: $20.00
Published on Web 05/24/2001

a qualitatively different temperature dependence. These latter dynamics are much faster and can be described by a time constant of about 10 ps, which is temperature independent up to almost 20 K above the phase transition. A similar result was obtained by OKE experiments[8] performed on 5CB. They are attributed to reorientation within the pseudonematic domains. The only theory predicting a temperature-independent component in liquid crystals was developed by Sengupta et al.[23] In it, the dynamics are analyzed in terms of the fluctuation modes of pseudonematic domains corresponding to length scales from a molecular size to the domain correlation length. Temperature-independent behavior is predicted to take place on small length scales.

The comparison of OKE experiments with solvation dynamics data and their common interpretation is possible only if the description of the dye molecules as probe molecules is correct, because specific interactions between dye molecule and solvent molecules may cause specific contributions to the solvation dynamics. In this work, we present measurements with a different member of the family of the alkylcyanobiphenyls to be able to expand our observations to the whole family of the alkylcyanobiphenyls. This homologue is butylcyanobiphenyl (4CB). The influence of the specific choice of the probe molecule was also investigated through measurements of the solvation dynamics with a chromophore very different from the cationic Rh700, namely, the neutral coumarin 153 (C153).

Together with the solvation dynamics data, we present experimental results on rotational dynamics of C153 in 8CB and compare them with the ones already obtained for Rh700 in 8CB. These experiments were performed to check the universality of the liquid crystalline solvation dynamics observed in our former investigations.

The solvation dynamics are monitored by transient Stokes shift measurements while reorientational dynamics are observed via time-resolved fluorescence anisotropy. Two different techniques have been used to record the fluorescence decays: fluorescence up-conversion and time-correlated single-photon-counting.

In the next section, the two sample systems Rh700 in 4CB and C153 in 8CB which have been investigated will be introduced, and the experimental setups will be described. To analyze the data, a procedure proposed by Maroncelli[14] was used. Its application to our system will be presented in section 3 together with the results. At the end of the section the analysis of the reorientational data will be presented. Section 4 is dedicated to the discussion of the experimental results. The temperature dependence of the relaxation times for the solvation dynamics in the isotropic phase approaching the nematic−isotropic phase transition is analyzed, and the different contributions are discussed. Special attention is given to the influence of the probe molecules. Concluding remarks are given in the last section.

Experimental Section

Both liquid crystalline materials 8CB (4′-*n*-octyl-4-cyanobiphenyl) and 4CB (4′-*n*-butyl-4-cyanobiphenyl) were purchased from MERCK England and were used without further purification. 8CB forms, besides the isotropic phase, the phase that has been investigated in the measurements presented here, a nematic phase between 306.5 and 313.5 K, a smectic A phase between 294.5 and 306.5 K and a crystalline phase below 294.5 K. 4CB in contrast does not form liquid crystalline phases since it experiences a monotropic isotropic−nematic phase transition at 289.15 K while it crystallizes 2 K above this temperature. The crystalline 4CB melts at 321 K. Spontaneous crystallization between 321 and 291 K made it impossible to measure the solvation dynamics of 4CB at more than three different temperatures in this temperature range. The purity of the liquids was tested by the agreement of the measured phase transition temperatures with the values listed in the literature.[24,25]

Two different probe molecules, rhodamine 700 (Rh700) and coumarin 153 (C153), were utilized. Both dyes were purchased from Lambda Physik and used as received. Rh700, which has been used already as probe molecule in the investigation of the solvation dynamics of 8CB,[18] is a cationic dye (counterion perchlorate), while C153 is a neutral molecule. For all the measurements, solutions of a concentration of $\sim 5 \times 10^{-4}$ mol/L were prepared. All measurements were performed in quartz sample cells of 2-mm optical path length. Strong degradation of the sample above 350 K, resulting in a fast decoloration of the solution, prevents the taking of data above this temperature.

The absorption spectra were recorded with an Uvikon 860 spectrometer from Kontron Instruments with a resolution of 1 nm. The sample was heated by means of a water-thermostat and the temperature was controlled by a Cr/Al-thermoelement (precision $\pm$ 0.5 °C).

The measurements of solvation dynamics for the system Rh700 in 4CB were performed using the fluorescence up-conversion technique (FluC). This experimental setup has been described elsewhere.[18] The excitation wavelength was 650 nm, and the temporal resolution was below 1.5 ps. The time window for the dynamics was limited by the optical delayline employed to a value of 6.7 ns. This time window was long enough to record the whole fluorescence decay, since the excited singlet state of Rh700 has a 3 ± 0.3 ns lifetime.

Analogous measurements for C153 in 8CB were performed using a completely different instrumentation. Since the fluorescent state of C153 has a long lifetime (5.6 ns), two different experimental techniques were employed to record the whole fluorescence decay: a FluC setup for the "fast" dynamics, and the time-correlated single-photon-counting (TCSCP) technique for the slower part of the decay.

To investigate the solvation dynamics, the time-resolved fluorescence is detected at different wavelengths under magic angle configuration. The rotational dynamics of C 153 was measured only with the TCSPC technique. It is independent of wavelength, but the fluorescence decays have to be recorded separately for parallel and perpendicular polarization of the excitation beam with respect to the detected light.

The FluC measurements were performed using a Spectra Physics Ti:sapphire laser system. The Tsunami 3960 produces ~80 fs pulses with a 82-MHz repetition rate and was run at 840 nm. The output was frequency doubled (Spectra Physics model 3980-4) to the excitation beam at 420 nm. For the measurements, excitation intensities of ~50 mW were chosen. The residual fundamental with an average power of 650 mW was used as gating pulse.

The excitation pulse was focused by means of a 50-mm lens into a 2-mm quartz cell containing the liquid solution. The fluorescence was collected by a Zeiss reflective microscope objective (52/0.66). The fluorescence collected by the microscope objective was recollimated by a 50-mm lens. The gate pulse was sent into a 15-cm delay line which allowed the observation of the evolution of the fluorescence intensity over 900 ps. The delay line was driven by a DC motor (Newport) with 1 μm resolution. In a beam splitter, the fluorescence and the gate pulses were superimposed and both beams were focused by a 25-mm lens into a 0.4-mm-thick type II BBO crystal

(Gsänger, Germany). Intensity and polarization of the excitation beam could be controlled through a combination of half wave plates and polarizers. The divergent up-conversion signal was collimated by a set of lenses and focused into a motor-driven double monochromator (Jobin Yvon H10-D-UV/VIS) with 1-nm resolution. The light at the selected wavelength was detected by a photomultiplier (Hamamatsu R4632). A 330-nm band-pass filter (Laser Components) was set in front of the monochromator to suppress efficiently the light at the fundamental wavelength. The excitation beam was chopped at 800 Hz, and the signal was sent into a lock-in amplifier (EG&G model 5209) connected to a computer. Signal averaging was achieved by collecting scans through repeated running of the delay line. This setup had a time resolution better than 1 ps. The temperature of the sample could be varied by a metal heating stage and was controlled by a Cr/Al-thermoelement with a precision of ± 0.5 °C. To avoid saturation effects, the sample was stirred and moved perpendicular to the optical axis. The TCSPC measurements could be performed parallel to the FluC measurements. About 10% of the 420 nm output of the frequency doubler was split off by a glass plate and sent into the TCSPC setup. The light was focused into the sample and the fluorescence was collected by a microscope objective (Zeiss Plan Neofluar X25/0.6) under an angle of ∼110°. A set of neutral density filters and polarizers in the excitation and detection beam paths allowed an independent choice of intensities and polarizations. A 435-nm long-pass-filter behind the microscope objective eliminates residual laserlight. The fluorescence was focused by a 10-mm lens into a motor-driven double monochromator (Jobin Yvon H10-D) with 1-nm resolution and detected by a microchannel-plate (Hamamtsu R3809U-51). The fluorescence photons were used as start-trigger on a TCSPC-PC card (Becker & Hickl SPC300), while a small part of the excitation light detected by a fast photodiode served as stop-trigger. The time resolution of this setup was ∼100 ps. The sample was heated by a continuous flow of hot air. The temperature was controlled by a Cr/Al thermoelement with a precision of ± 0.5 °C.

The steady-state fluorescence spectrum of Rh700 in 4CB was recorded with a National Instruments PC-card (Labpc 1200 AI) with an excitation wavelength of 632.8 nm. C153 in 8CB was excited at 442 nm, and the detection unit for the fluorescence spectrum consisted of a doublemonochromator (SPEX 1402), a Hamamatsu photomultiplier (C31034), a Stanford Research preamplifier (SR440), and single-photon-counter (SR400).

Data Analysis and Results

The goal of the data analysis is to reconstruct the fluorescence spectra at different times from the temporal evolution of the fluorescence intensities recorded at different wavelengths of the fluorescence spectra. The solvation dynamics can then be read off the temporal evolution of the spectra. A short account of this reconstruction procedure will be given. For a more detailed discussion, the literature[14,17−19,26] should be consulted.

Figure 1 shows the temporal evolution of the fluorescence intensity of C153 in 8CB at 42 °C and at two different wavelengths (up-conversion wavelengths 306 and 324 nm correspond to fluorescence wavelengths of 481 and 527 nm, respectively). The data in the first 850 ps are obtained by the FluC technique, while at later times the decays were measured via TCSPC. Since in the time window of ∼12 ns the fluorescence has not completely decayed, the data were corrected to eliminate the contribution of residual fluorescence of the preceding pulse. The inset shows the evolution of the first 500 ps. The obvious wavelength dependence displayed by the form

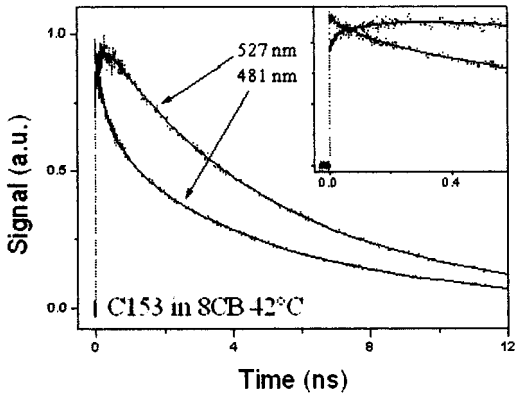

Figure 1. Normalized fluorescence decays of 5×10^{-4} M C153 in 8CB at 42 °C and for two different fluorescence wavelengths on the blue (481 nm) and red (527 nm) edge of the steady-state fluorescence spectrum. The first 850 ps were observed by the fluorescence up-conversion technique, while at later times the decays were measured with the TCSPC technique. The inset shows the evolution of the signal in the first 500 ps.

of the two decays is a clear indication of the solvation process. The straight lines in Figure 1 ($I(\upsilon,T)$) are the results of a multiexponential fit of the experimental data. A more thorough analysis performed on some data sets, making use of deconvolution of the signal from the rising part of the signal, did not show any substantial change in the decay time constants of the multiexponential fit. As a consequence, the deconvolution procedure was not applied in the data analysis presented here. The C153 data are well fitted by a sum of four exponential functions, while the Rh700 data could be described by a triple exponential function. The need of an additional decay parameter for the C153 data can be ascribed to the longer lifetime of C153 compared to Rh700. The longer accessible time window allows a clearer detection of solvation dynamics processes occurring on a nanosecond time scale. Since all decays were measured independently, the intensities of the different curves are not directly related. To reconstruct the fluorescence spectra at different times, it is necessary to normalize these intensities. This is achieved by means of the following formula

$$F(\upsilon,t) = \frac{I(\upsilon,t)I_0(\upsilon)}{\int_0^\infty I(\upsilon,t)dt} \tag{1}$$

where $I_0(\upsilon)$ is the steady-state fluorescence spectrum.

Figure 2 shows the absorption and fluorescence spectra of Rh700 in 4CB and C153 in 8CB. The fluorescence spectrum of Rh700 exhibits a clear vibrational structure. Its first maximum can be described by a Gaussian peak function (full line) and was the one used in monitoring the solvation dynamics. The fluorescence spectrum of C153 does not display a distinct vibronic structure and is well fitted by a log-normal function (full line). The time-dependent fluorescence intensity was measured for Rh700 at eight different wavelengths and for C153 at up to 19 wavelengths due to the broader spectrum of C153.

The maximum $\upsilon_{max}(t)$, which is used as the indicator of the solvation dynamics, can be determined by fitting the reconstructed fluorescence spectra $F(\upsilon,t)$ from eq 1 at different times t to the functional form employed for the steady state fluorescence spectra.

The temporal evolution of $\upsilon_{max}(t)$ at different temperatures shows a multiexponential behavior, which can be fitted for the system C153 in 8CB systematically by a triple exponential function (eq 2):

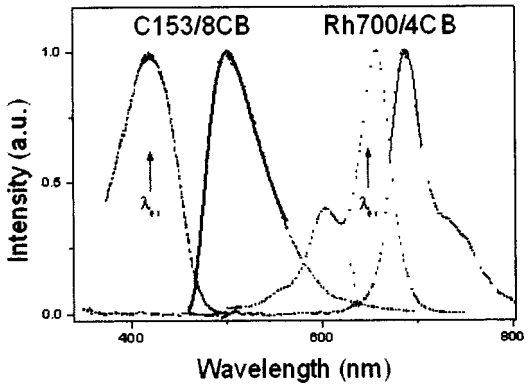

Figure 2. Absorption and fluorescence of a 5×10^{-4} M solution of C153 in 8CB and of Rh700 in 4CB in the isotropic phase of 8CB and 4CB, respectively. The solid lines reflect $I_0(\nu)$ used in the spectral reconstruction of the time-resolved fluorescence spectra. Additionally, the excitation wavelengths for the up-conversion experiments are shown.

$$\nu_{max}(t) = A_{fast}\exp(-t/\tau_{fast}) + A_{middle}\exp(-t/\tau_{middle}) + A_{slow}\exp(-t/\tau_{slow}) + \nu_{max}(\infty) \quad (2)$$

The shift for the system Rh700 in 4CB is less systematic. As observed in the earlier measurements on Rh700 in 8CB, the slowest component cannot always be detected; therefore, only the two faster components will be analyzed for this chromophore. The normalized spectral response function $S_v(t)$ was calculated according to equation:

$$S_v(t) \equiv \frac{\nu_{max}(t) - \nu_{max}(\infty)}{\nu_{max}(0) - \nu_{max}(\infty)} \quad (3)$$

The values of $\nu_{max}(t)$ after 1 ps and extrapolated to time infinity were used as $\nu_{max}(0)$ and $\nu_{max}(\infty)$, respectively. The $S_v(t)$ curves at three different temperatures are depicted in Figure 3 for the system Rh700 in 4CB and in Figure 4 for C153 in 8CB, respectively. The Stokes shift detected was 100 ± 20 cm^{-1} and 500 ± 50 cm^{-1} for Rh700 in 4CB and C153 in 8CB, respectively. These parameters did not show a clear temperature-dependent behavior. The difference in the value for the two chromophores is attributed to the bigger change in dipole moment upon excitation for C153 with respect to Rh700.

The $S_v(t)$ curves were fitted with multiexponential decays as well. The fit parameters are collected in Table 1 for C153 in 8CB and in Table 2 for Rh700 in 4CB. While the amplitudes of the different terms are essentially constants at the various temperatures, the decay times show a dependence from temperature, which will be considered in details in the following.

The temperature dependence of the time constants characterizing the slowest component (τ_{slow}) for C153 in 8CB are presented in Figure 5, while Figure 6 shows the same data for the intermediate (τ_{middle}) component for both C153 in 8CB and Rh700 in 4CB. The temperature dependence of the relaxation times is displayed as a function of the distance from the nematic−isotropic phase transition temperature T_{NI}. τ_{slow} has values in the range of several hundreds of picoseconds, and τ_{middle} is an order of magnitude smaller. Both these components show a clear temperature dependence. It is important to point out that the values of τ_{middle} for the two different chromophores are of the same order of magnitude. One has also to mention that the values of τ_{slow} are comparable to the lifetime of the chromophore. The latter one has not been fixed in the fit of the original fluorescence decays. As a consequence, the error associated with τ_{slow} is much larger than the error affecting τ_{middle} and τ_{fast}.

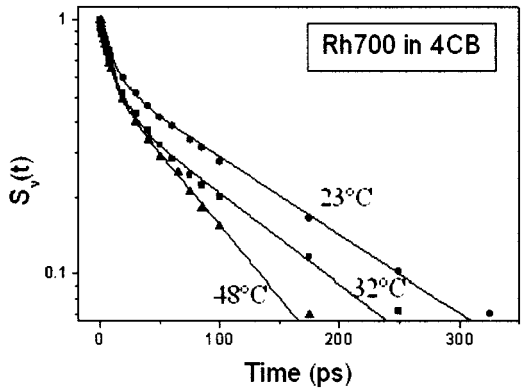

Figure 3. Spectral response function $S_v(t)$ (see text) for 5×10^{-4} M Rh700 in 4CB at three different temperatures. The lines are the result of a double exponential fit of the $S(t)$ curves.

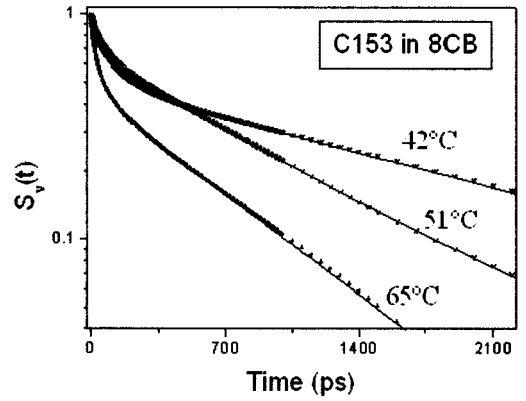

Figure 4. Spectral response function $S_v(t)$ (see text) for 5×10^{-4} M C153 in 8CB at three different temperatures. The lines are the result of a triple exponential fit of the $S(t)$ curves.

TABLE 1: Fit Parameters of $S_v(t)$ for C153 in 8CB

temp (K)	A (fast)	τ (fast)	A (middle)	τ (middle)	A (slow)	τ (slow)
315	0.14	8.7	0.36	111	0.49	1961
320	0.07	13	0.27	107	0.64	804
324	0.1	11	0.25	75	0.64	886
329	0.16	12	0.42	96	0.42	1245
334	0.16	10	0.3	68	0.44	382
338	0.21	12	0.33	54	0.44	668

[a] A = amplitude (a.u.) and τ = time (ps).

TABLE 2: Fit Parameters of $S_v(t)$ for Rh700 in 4CB

temp (K)	A (fast)	τ (fast)	A (middle)	τ (middle)
296	0.45	11.8	0.55	142
305	0.46	11.8	0.54	122
314	0.46	8	0.54	93
321	0.46	8.3	0.54	75
322	0.53	10	0.47	50
330	0.54	3.6	0.46	29
333	0.14	1.7	0.86	15
336			1	8

[a] A = amplitude (a.u.) and τ = time (ps).

The solid lines in Figures 5 and 6 are the result of a fit of the solvation time constants according to equation:

$$\tau_{solvation} = A\frac{\eta(T)}{T} \quad (4)$$

where $\eta(T)$ is the viscosity of 8CB and 4CB, respectively, and

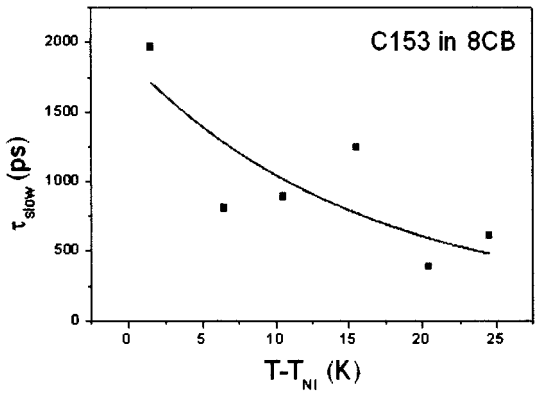

Figure 5. Decay time τ_{slow} (squares) for the slowest component of $S_v(t)$ (see text) as a function of $(T-T_{NI})$ for C153 in 8CB. The solid line is the result of a fit according to eq 4. The activation energy for the viscosity is $E_a = 48 \pm 18.5$ kJ/mol.

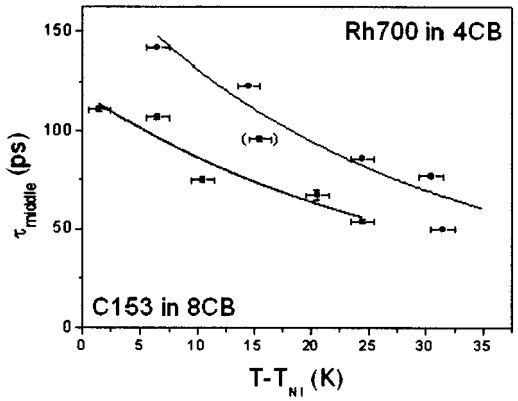

Figure 6. Decay times τ_{middle} of $S_v(t)$ (see text) as a function of $(T-T_{NI})$ for C153 in 8CB (squares) and Rh700 in 4CB (circles). The solid lines are the result of a fit according to eq 4. The activation energies for the viscosity are E_a (8CB) $= 24.5 \pm 5.4$ kJ/mol and E_a (4CB) $= 25 \pm 4.5$ kJ/mol.

T is the temperature. This functional correlation is predicted by the theory of polar solvation. The activation energies of the viscosity obtained by the fit procedure are the following: τ_{slow}(C153/8CB) 48 ± 18.5 kJ/mol, τ_{middle}(C153/8CB) 24.5 ± 5.4 kJ/mol, τ_{middle}(Rh700/4CB) 25 ± 4.5 kJ/mol. For Rh700/8CB, a value of 25 ± 3 kJ/mol had been found,[18] and in the literature a value of 31.8 kJ/mol for pure 8CB[24] has been reported.

The temperature dependence of the fastest component plotted versus $(T-T_{NI})$ is shown in Figure 7 for both sample systems. In either case, the relaxation time (τ_{fast}) has an absolute value of ~10 ps. This component is temperature independent up to ~20 K above the nematic−isotropic phase transition. The dashed line is a guide to the eye to emphasize this behavior.

In addition to the solvation dynamics the rotational dynamics of Rh700 and C153 in 8CB should be compared. The rotational relaxation times were determined at different temperatures by recording the time-resolved fluorescence anisotropy $r(t)$[27]

$$r(t) = \frac{I_{II}(t) - I_{\perp}(t)}{I_{II}(t) + 2I_{\perp}(t)} \tag{5}$$

$I_{II}(t)$ and $I_{\perp}(t)$ are the intensities of the time-resolved fluorescence measured by exciting the system with a polarization parallel or perpendicular to the detected light, respectively. The experimental curves for C153 in 8CB at 65 °C are shown in Figure 8. Since $I_{II}(t)$ and $I_{\perp}(t)$ were recorded independently it is

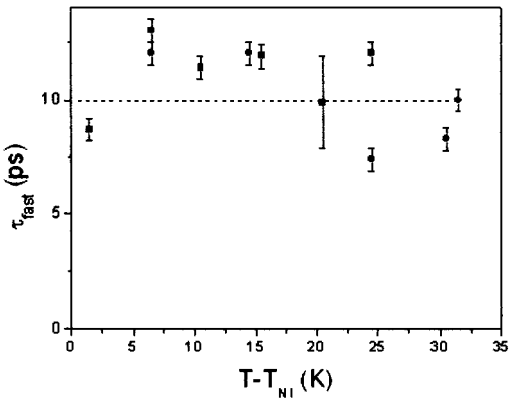

Figure 7. Decay time τ_{fast} (squares) for the fastest component of $S_v(t)$ as a function of $(T-T_{NI})$ for C153 in 8CB (squares) and Rh700 in 4CB (circles). A guide to the eye (dashed line) to emphasize the temperature-independent behavior is added.

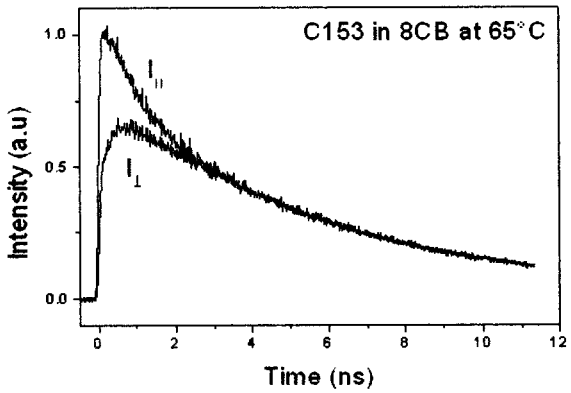

Figure 8. Fluorescence decays measured at parallel (I_{II}) and perpendicular polarization ($I_{\perp}$) for C 153 in the isotropic phase of 8CB at 65 °C.

necessary to determine their relative intensities to calculate $r(t)$. To this end, the tail matching method was used.

The data of Rh700 in 8CB have been published[18] before, but a new data analysis was performed resulting in slightly slower relaxation times. The $r(t)$ curves for both chromophores obtained by means of this procedure were fitted by a double exponential function and the average time constants were determined. The contributions of the two relaxation times were weighted by their respective amplitudes. In Figure 9 the temperature dependence of the rotational relaxation times τ_{or} is presented. The solid lines in Figure 9 are the result of a fit with the formula

$$\tau_{or} = B\frac{\eta(T)}{T} \tag{6}$$

where $\eta(T)$ is the viscosity of 8CB and T is the temperature. The Debye−Stokes−Einstein (DSE) model predicts this temperature dependence and activation energies of 28.1 ± 2.4 k/mol for Rh700 in 8CB and 30.2 ± 2.9 kJ/mol for C153 in 8CB are obtained.

Discussion

In an earlier paper,[18] we have presented the results of the solvation dynamics found for Rh700 in 8CB. In that system, two different relaxation processes were found. The slower one in the range of 100 ps could be attributed to polar solvation and was characterized by a distinct temperature dependence. The second process, which was temperature independent up to 20 K above the isotropic−nematic phase transition, was

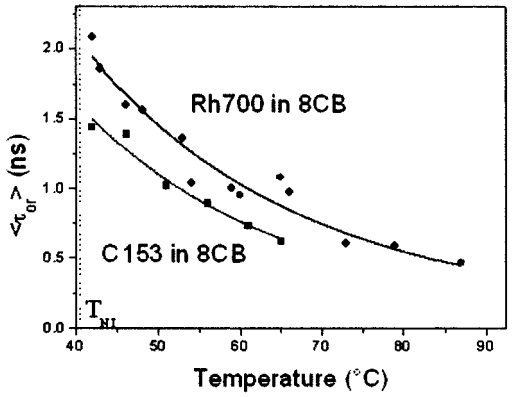

Figure 9. Temperature dependence of the average decay time constant $\langle\tau_{or}\rangle$ of the fluorescence anisotropy $r(t)$ of Rh700 in 8CB and C153 in 8CB. The solid line is the result of a fit to eq 5. From the fits the viscosity activation energies E_a (Rh700) = 28.1 ± 2.4 kJ/mol and E_a (C153) = 30.2 ± 2.9 kJ/mol are obtained. The dashed line indicates the temperature at which the nematic−isotropic phase transition occurs.

explained in terms of the liquid crystalline properties of the solvent. Yet, it could not be excluded that a special interaction between solute and solvent occurred, which may arise by coupling of the positive charge of the Rh700 molecule and the dipolar solvent molecules.

The solvation dynamics of Rh700 in 4CB have been measured to be able to compare the solvation dynamics for two different homologues of the alkylcyanobiphenyl family. For this system, we expect very similar results to those found for Rh700 in 8CB. Figures 6 and 7 show that this is indeed the case. The two components display the same characteristic features, so it can be concluded that this behavior is common to the whole family of alkylcyanobiphenyls.

The central goal of the work presented in this publication was the understanding of this temperature-independent component. Up to now, there exists no theoretical work about solvation dynamics of liquid crystals, which could explain this temperature-independent contribution, so our experimental results will be discussed in the framework of the experimental work performed by other groups on liquid crystals.

C153 and Rh700 are very different probe molecules especially concerning their electronic properties. C153 is a neutral molecule while Rh700 carries a positive charge. The experimental results obtained for the solvation dynamics of 8CB with the probe molecule C153 should reflect clearly whether the temperature-independent component is a general characteristic of the solvent alkylcyanobiphenyl or if it has to be assigned to a specific interaction between the ionic chromophore Rh700 and the solvent molecules. Figure 7 shows clearly that the absolute value of the fastest relaxation time for the solvation process of C153 is with ∼10 ps practically identical to the corresponding component found for Rh700. It follows that we can ascribe this temperature-independent process to the general characteristics of the nematogenic solvents.

Our experiments show that it is indeed correct to consider the dye molecules just as probe molecules which do not influence the fast dynamics of the liquid crystalline host. There is a number of experimental results which support the idea that this temperature-independent component is a direct result of liquid crystalline interaction of the solvent molecules. All these observations have in common that temperature-independent processes are observed and are attributed to local ordering.

OKE measurements with subpicosecond time resolution performed on bulk 5CB[8] and MBBA[9] in the isotropic phase show a similar behavior. In the picosecond range, the OKE signal measured in these liquids is characterized by a strongly nonexponential decay which is temperature-independent up to 30 K above the phase transition. This nonexponential decay is explained in terms of relaxation on a short length scale within the long range orientationally correlated pseudonematic domains.

Infrared spectroscopic investigations have been performed on 8CB in the different phases.[28] Two signals at 15−50 and 95−110 cm^{-1} do not vary significantly even if the temperature or phase are changed. These bands are interpreted as librations and torsional motions of parts of the molecules. Local ordering persistent on the time scale of these motions is used to account for this temperature independence.

Finally, the presence of a pronounced local order in the isotropic phase of liquid crystals has been shown in X-ray diffraction experiments.[29] Leadbetter et al. have observed structures formed by about 50 molecules reminding of smectic order in the nematic phase of 5CB and 7CB. The signals related to this locally ordered structure do not vanish even in the isotropic phase.

If local ordering also exists in the immediate surroundings of the chromophore, molecular dynamics within this structured liquid will evolve in an anisotropic potential and the molecule may relax in a quasi-static environment, quite analogous to the interpretation of the vibrational data. It is important to point out that the processes observed in these various experiments are probably not identical, but the growing number of experimental results which observe temperature-independent dynamics in the isotropic phase of nematogenic liquids strongly indicate the local order as a common cause.

Another evidence for the proposed interpretation would be the comparison of the present results with solvation dynamics data of C153 in ordinary polar solvents. Unfortunately, to our knowledge, there is not a thorough study on this subject. The only temperature-dependent data are those reported by Maroncelli and Fleming,[26] in which they measure the solvation dynamics of C153 in *n*-propanol and propylene carbonate at five and three different temperatures, respectively. They fit the $S_v(t)$ curves with a multiexponential function and all the decay time constants show a marked temperature dependence, even in the tens of picosecond range. These findings would be a further proof of our interpretation for the fast component. A final word of caution has to be spent: the time resolution of the experiments performed in the paper just mentioned is claimed to be 30 ps, so the 10 ps data they report are affected by a large error.

We proceed now with the discussion of the temperature-dependent processes observed in the solvation dynamics measurements. 8CB and 4CB are polar liquids with a dipole moment of about 5 D.[30,31] For polar liquids solvation dynamics are normally described in terms of polar interactions expressed through the frequency-dependent dielectric constant $\epsilon(\omega)$

$$\epsilon(\omega) = \epsilon_\infty + \frac{\epsilon_0 - \epsilon_\infty}{1 - i\omega\tau_D} \tag{7}$$

where ϵ_0 and ϵ_∞ are the static and infinite frequency dielectric constants and τ_D is the Debye relaxation time. The time-dependent Stokes shift for a single Debye dispersion regime as implied in eq 7 is described[32,20,21] by a monoexponential function with a time constant τ_F approximately given by

$$\tau_F = \left(\frac{\epsilon_\infty}{\epsilon_0}\right)\tau_D \tag{8}$$

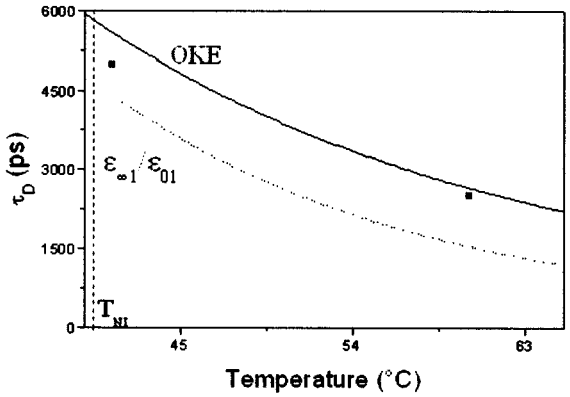

Figure 10. Comparison of solvation dynamics relaxation times τ_{slow} of C153 in 8CB with reorientational dynamics results obtained from dielectric measurements[12] (squares) and OKE experiments[8] (solid line). For a clearer presentation, the corresponding values of the fit function in Figure 5 instead of the data points are displayed (dotted line). For the explanation see the text.

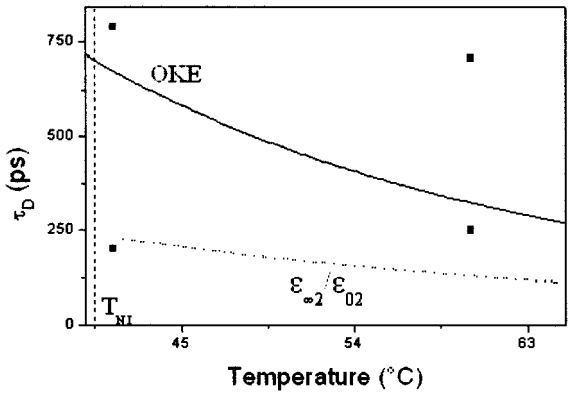

Figure 11. Comparison of solvation dynamics relaxation times τ_{middle} of C153 in 8CB with reorientational dynamics results obtained from dielectric measurements[12] (squares) and OKE experiments[8] (solid line). For a clearer presentation, the corresponding values of the fit function in Figure 5 instead of the data points are displayed (dotted line). For the explanation see the text.

If the dielectric constant displays more than one dispersion regime several characteristic relaxation times are predicted for solvation dynamics.[21]

Equation 8 offers the possibility to compare the reorientational relaxation times τ_D with the solvation times τ_F. There are different ways to determine τ_D; the most direct method being high-frequency dielectric measurements. These measurements, performed on 8CB, have shown three different time constants.[12] In the isotropic phase, their values lie in the range of 200, 750, and 4000 ps. The values at two different temperatures are shown in Figure 10 and Figure 11 (square symbols). Alternatively, the reorientational times τ_D can be determined by optical Kerr effect (OKE) measurements. Since the OKE measurements of pure 8CB do not give information about single molecule reorientation, we used the relaxation times Deeg et al.[8] obtained for a 0.66 mol/L 5CB (4′-*n*-pentyl-4-cyanobiphenyl)/*n*-heptane mixture by the same experiment. In those measurements, no collective reorientation is observed and the induced anisotropy is destroyed by reorientation of isolated 5CB molecules. The results have been used assuming that the reorientational times for 5CB and 8CB are comparable due to their similar molecular structure. Deeg et al. observed two relaxation times for the reorientation of 5CB in *n*-heptane. Both relaxation times are characterized by a DSE temperature dependence. From a theoretical point of view, the reorientational time τ_R measured with the OKE technique is three times faster than τ_D. On the other hand, experiments performed on nitrobenzene and bromobenzene with OKE and dielectric measurements have shown that $\tau_R \approx \tau_D$,[37] so that we will consider $\tau_R = \tau_D$. From those data, the relaxation times τ_D have been extrapolated to the viscosity regime of our measurements. The temperature dependence of the viscosity of 8CB is known and the extrapolated curves can be shown as a function of temperature (solid lines in Figures 10 and 11). The slower time constant agrees very well with the slowest component found in the dielectric experiments, while the faster component of the OKE measurements lies between the two faster dielectric relaxation times. These data obtained with two different methods do not completely coincide, but they allow the estimation of whether the two components observed for the solvation dynamics of C153 in 8CB may be explained in terms of Debye rotational times. To compare our experimental results with the experimental findings described above, the experimentally measured τ_F have to be converted into τ_D through eq 8. To this end, the values of ϵ_0 and ϵ_∞ are needed for the different dispersion regimes. From the dielectric measurements of Druon et al.[11] the following rough estimates: $\epsilon_{01} = 9.5$, $\epsilon_{\infty 1} \approx 3.8$ and $\epsilon_{02} = 5$, $\epsilon_{\infty 2} \approx 2.5$ have been calculated. The dotted lines in Figures 10 and 11 are the result of the application of eq 8 to the solid lines depicted in Figures 5 and 6, respectively (obtained by fitting our experimental IF data). The values for the slower component agree very well. For the faster component, the solvation data result in values which are a factor of 3 smaller than the values found for the OKE estimations and lie in the range of the faster dielectric data points. Considering the crude approximations necessary to make this comparison, this agreement is quite acceptable, and we conclude that these components are indeed the result of dielectric relaxation.

With the background of this assumption an obvious difficulty arises for the interpretation of the Rh700 data where only one clearly temperature-dependent component could be detected. We cannot unequivocally solve this discrepancy, but there are different possible explanations. The first one takes into consideration that the data analyses employed make it difficult to extract solvation times comparable to the fluorescence lifetime. Rh700 has a fluorescence lifetime which is a factor of 2 shorter than the lifetime of C153 comparable to the slowest relaxation component found for C153. The second explanation takes into account the fact that polar solvation does not predict any dependence of the observed solvation relaxation times from the probe molecule. Although we demonstrated the small influence of the nature of the probe molecule above, we cannot completely rule out the possibility that the ionic chromophore Rh700 has a small orienting influence on the solvent weakening one of the temperature-dependent solvation components seen for C153. To test this hypothesis, further measurements of solvation dynamics with ionic dyes of longer fluorescence lifetimes in 8CB have to be carried out.

Parallel to the solvation dynamics the rotational dynamics of the probe molecules Rh700 in 8CB and C153 in 8CB were investigated. Rotational dynamics data are normally interpreted in terms of the Debye−Stokes−Einstein (DSE) theory. (a detailed description can be found in the literature[33−36]). Simple DSE theory assumes so-called "stick" boundary conditions with a first solvent shell attached to the rotating molecule. Experimentally, these conditions seem to hold only for systems where the rotating body is at least three times larger[37] than the solvent molecules. For smaller ratios the rotation is faster and takes

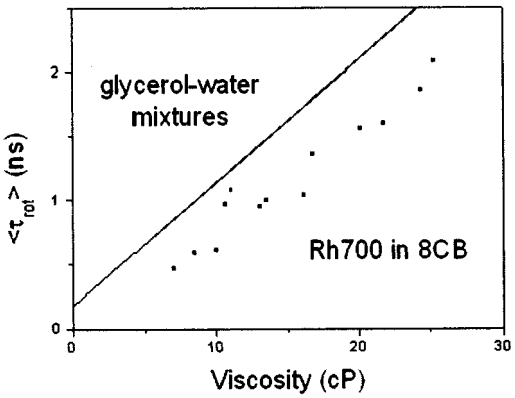

Figure 12. Comparison of reorientational relaxation times τ_{or} of Rh700 in 8CB (squares) with corresponding values obtained for Rh700 in different glycerol−water mixtures[40] (solid line).

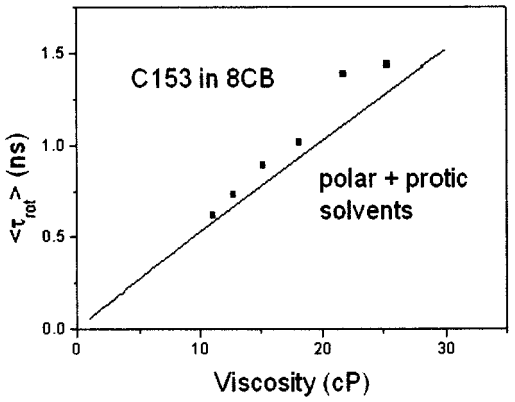

Figure 13. Comparison of reorientational relaxation times τ_{or} of C153 in 8CB (squares) with those obtained for C153 in other liquids[39] (solid line representing the fit to the experimental data).

place under "slip" boundary conditions[38] with no solvent molecules attached to the rotating molecule.

The sizes of C153, Rh700, and 8CB have been estimated to be 246 Å^3,[39] 310 Å^3,[40] ∼300 Å^3, respectively, and "slip" boundary conditions are expected. In Figure 12 and 13 rotational relaxation data are depicted as a function of solvent viscosity. The solid lines in the two figures represent rotational relaxation times for Rh700 in different glycerol−water mixtures[40] (Figure 12) and for C153 in a large number of different polar solvents[39] (Figure 13) taken from literature. Our experimental values for the solvent 8CB are represented by squares in both figures. They are somewhat faster than the literature values for Rh700 (Figure 12) and slightly slower for C153 (Figure 13). However, whereas "slip" boundary conditions are expected for 8CB, the solvents used for the literature data should fall under under "stick" boundary conditions and display considerably slower times than the data found for 8CB. The fact that this is clearly not the case strongly indicates that the description of the solvent as a continuum and the rotation of the probe molecule only governed by hydrodynamic flow does not hold for this complex nematogenic solvent. The difference between the reorientational times of Rh700 and C153 can be attributed to a pure size effect although an influence of chromophore charge as, for example, found for neutral red,[41] cannot be completely ruled out.

Conclusions

We have investigated the solvation dynamics of Rh700 in the isotropic phase of 4CB and of C153 in the isotropic phase of 8CB. These measurements have been extending earlier investigations on the system Rh700 in 8CB to gain a better understanding of the solvation dynamics in liquid crystalline materials. The results found for the system Rh700 in 4CB show clearly that the peculiar behavior observed for the system Rh700 in 8CB is common to all members of the family of the alkylcyanobiphenyls. Two distinct processes between 1 and 500 ps characterize its solvation dynamics. The faster process is temperature-independent above the nematic−isotropic phase transition with a relaxation time constant of ∼10 ps. The slower process, characterized by a time scale of 100 ps, fits into the picture of polar solvation and shows the typical temperature dependence for Debye relaxation.

To investigate the possible influence of the specific probe molecule chosen the system C153 in 8CB was investigated. The fastest solvation component in this sample is practically identical to the one detected with Rh700. This allows the interpretation of this component as a characteristic feature of the dynamics of alkylcyanobiphenyls. We believe that this component is a consequence of specific liquid crystalline interactions, since other experiments as OKE, vibrational and X-ray spectroscopy show temperature-independent contributions to the dynamics of nematogenic substances as well, and these results are explained by local ordering in the liquid. Besides this temperature-independent component, slower contributions with a distinct temperature dependence are observed in all samples. This behavior can be attributed to polar solvation. One of these components relaxing with time constants in the range of 100 ps has been found for both chromophores, Rh700 and C153. A second temperature-dependent component in the nanosecond time range only observed reliably in the sample C153 in 8CB is also associated with polar solvation. If this component depends on the probe molecule or is due to different boundary conditions for the data analysis could not be clarified with the available data. Reorientational dynamics measurements of Rh700 and C153 in 8CB show relaxation times very similar to those found in solvents with considerably smaller molecular size. This is surprising since "stick" contributions are expected for those solvents, whereas "slip" boundary conditions and considerably faster relaxation times should hold for 8CB.

Acknowledgment. We thank the Deutsche Forschungsgemeinschaft for financial support of this work under De446/2-2.

References and Notes

(1) Stinson, T. W.; Litster, J. D. *Phys. Rev. Lett.* **1970**, *25*, 503.
(2) Coles, H. J. *Mol. Cryst. Liq. Cryst. (Lett.)* **1978**, *49*, 67.
(3) Wong, G. K. L.; Shen, Y. R. *Phys. Rev. Lett.* **1973**, *30*, 895.
(4) Gierke, T. D.; Flygare, W. H. J. *Chem. Phys.* **1974**, *61*, 2231.
(5) (a) de Gennes, P. G. *Physics Lett.* **1969**, *30A*, 454; (b) de Gennes, P. G. *Mol. Cryst. Liq. Cryst. (Lett)* **1971**, *12*, 193.
(6) Stinson, T. W.; Litster, J. D. *Phys. Rev. Lett.* **1973**, *30*, 688.
(7) Courtens, E.; Koren, G. *Phys. Rev. Lett.* **1975**, *35*, 1711.
(8) Deeg, F. W.; Greenfield, S. R.; Stankus, J. J.; Newell, V. J. Fayer, M. D. *J Chem. Phys.* **1990**, *93*, 3503.
(9) Stankus, J. J.; Torre, R.; Fayer, M. D. *J. Phys. Chem.* **1993**, *97*, 9478.
(10) Rizi, V.; Ghosh, S. K. *Il Nouv. Cim.* **1993**, *15D (4)*, 661.
(11) Druon, C.; Wacrenier, J. M. J. *Phys. (Paris)* **1987**, *38*, *47*.
(12) Bose, T. K.; Chahnine, R.; Merabet, M.; Thoen, J. J. *Phys. (Paris)* **1984**, *45*, 1329.
(13) Bose, T. K.; Campbell, B.; Yagihara, S.; Thoen, J. *Phys. Rev. A* **1987**, *86*, 5767.
(14) Horng, M. L.; Gardecki, J. A.; Papazyan, A.; Maroncelli, M. *J. Phys. Chem.* **1995**, *85*, 784.
(15) Reynolds, L.; Gardecki, J. A.; Frankland, S. J. V.; Horng, M. L.; Maroncelli, M. J. *Phys. Chem.* **1996**, *100*, 10337.
(16) Cichos, F.; Willert, A.; Rempel, U.; von Borczyskowski, C. *J. Phys. Chem. A* **1997**, *101*, 8179.
(17) Fourkas, J. T.; Benigno, A.; Berg, M. *J. Chem. Phys.* **1993**, *99*, 8552.

(18) Rau, J.; Ferrante, C.; Deeg, F. W.; Bräuchle, C. *J. Phys. Chem. B* **1999**, *103*, 931.
(19) Saielli, G.; Polimeno, A.; Nordio, P. L.; Bartolini, P.; Ricci, M.; Righini, R. *J. Chem. Soc., Faraday Trans.* **1998**, *94(1)*, *121*.
(20) van der Zwan, G.; Hynes, J. T. *J. Chem. Phys.* **1985**, *89*, 4181.
(21) Bagchi, B.; Oxtoby, D. W.; Fleming, G. R. *Chem. Phys.* **1984**, *86*, 257.
(22) Wolynes, P. G. *Annu. Rev. Phys. Chem.* **1980**, *31*, 345.
(23) Sengupta, A.; Fayer, M. D. *J. Chem. Phys.* **1995**, *102 (10)*, 4193.
(24) Kneppe, H.; Schneider, F.; Sharma, N. K. *Ber. Bunsen-Ges. Phys. Chem.* **1981**, *85*, 784.
(25) Product information MERCK (England).
(26) Maroncelli, M.; Fleming, G. R. *J. Chem. Phys.* **1987**, *86*, 6221.
(27) Fleming, G. R. *Chemical Applications of Ultrafast Spectroscopy*; Oxford University Press: New York, 1986.
(28) Vij, J. K.; Murthy, U. M. S. *J. Mol. Liq.* **1989**, *43*, 109.
(29) Leadbetter, A. J.; Richardson, R. M.; Colling C. N. *J. Physique* **1975**, *36*, C1−37.
(30) Cumber, C. W. N.; Dev, S. K.; Landoe, S. R. *J. Chem. Soc., Perkins. Trans. II* **1973**, *46*, 537.
(31) Dunmur, D. A.; Miller, W. H. *Mol. Cryst. Liq. Cryst.* **1980**, *60*, 281.
(32) Mazurenko, Yu. T. *Opt. Spectrosc. (USSR)* **1974**, *36*, 283.
(33) Debye, P. *Polar Molecules;* New York: Dover, 1928.
(34) Stokes, G. *Trans. Cambridge Philos. Soc.* **1985**, *9*, *5*.
(35) Einstein, A. *Ann. Physik (Leibzig)* **1906**, *19*, 289.
(36) Cantor, C. R.; Schimmel, P. R. *Biophysical Chemistry II*, W. H. Freeman & Company, New York, 1980.
(37) Böttcher, C. J. F.; Bordevijk P. *Theory of Electric Polarization*, Vol. II, 2nd ed.; Elsevier: Amsterdam, 1978.
(38) Hu, C.; Zwanzig, R. *J. Chem. Phys.* **1974**, *60*, 4354.
(39) Horng, M. L.; Gardecki, J. A.; Maroncelli, M. *J. Phys. Chem. A* **1997**, *101*, 1030.
(40) Megens, M.; Sprik, R.; Wegdam, G. H.; Lagendijk, A. *J. Chem. Phys.* **1997**, *107*, 493.
(41) Dutt, G. B.; Singh, M. K.; Sapre, A. V. *J. Chem. Phys.* **1998**, *10*, 5994.